Case Studies in Thermal Engineering 47 (2023) 103080

Contents lists available at ScienceDirect

Case Studies in Thermal Engineering

journal homepage: www.elsevier.com/locate/csite

Numerical study of heat transfer and melting process in a NEPCM filled 3D cuboid cavity: Application non-uniform temperature

Tarek Bouzennada [a], Kaouther Ghchem [b], Nesrine Zahi [c,d], Muapper Alhadri [e], Lioua Kolsi [e,f,*]

[a] Mechanical Engineering Department, Echahid Cheikh Larbi Tebessi University, Road of Constantine 12022, Tebessa, Algeria
[b] Department of Industrial Engineering and Systems, College of Engineering, Princess Nourah bint Abdulrahman University, P.O. Box 84428, Riyadh, 11671, Saudi Arabia
[c] Applied College, Huraymila, Imam Mohammad Ibn Saud Islamic University (IMSIU), Riyadh 11432, Saudi Arabia
[d] Laboratory of Thermal and Energy Systems Studies (LESTE), National Engineering School of Monastir (ENIM), University of Monastir, Avenue Ibn El Jazzar, 5019 Monastir, Tunisia
[e] Department of Mechanical Engineering, College of Engineering, University of Ha'il, Ha'il City, 81481, Saudi Arabia
[f] Laboratory of Meteorology and Energy Systems, University of Monastir, Monastir, 5000, Tunisia

ARTICLE INFO

Keywords:
Melting
Fusion
Nano-enhanced-PCM
3D numerical simulation

ABSTRACT

In this numerical study, a cubic box filled with a Nanoparticle Enhanced Phase Change Material (NEPCM) (mixture "N-Octadecane/alumina (Al_2O_3)"), is considered. Using Comsol-Multiphysics program, the configuration is treated as a 3D symmetric numerical simulation problem under fixed boundary conditions. Besides, heat transfer fluid (HTF) generates a non-uniform temperature that varies linearly along an internal tube installed in the lowest area of the enclosure to ensure the melting of the NEPCM. Therefore, the purpose of the study is to highlight the effect of the nanoparticles volume fraction (varying from 0 to 6%) on thermal distribution and melting performances. The obtained findings figure out that the PCM melts irregularly and is affected by the non-uniform temperature of the HTF tube. Hence, the third dimension should be considered, particularly in PCM ring tank simulations, in order to obtain reliable predictions compared to practical and experimental studies. Additionally, the Al_2O_3 nanoparticles have a valuable effect on improving the thermal conductivity of NEPCM, where thermal resistance and melting time are reduced with the increase of the nanoparticles volume fraction. Compared to the case of pure PCM, the heat transfer enhancement yields to an augmentation in the melting rate by about 11% and 9.5% for the volume fractions of 6% and 3%, respectively. Moreover, there is a significant increase in the amount of stored thermal energy when nanoparticles are dispersed in the PCM.

1. Introduction

Thermal energy storage using Phase Change Materials (PCMs) has gained attractiveness in many applications such as electronic components cooling [1], building's thermal insulation [2], thermal energy storage (TES) systems [3], etc. Recently, the scientific community has been seeking opportunities to expand the range of uses for these materials. While PCMs are primarily used as a result of their high thermal capacity, the limited thermal conductivity of PCMs presents a challenge for using them. Various refinement

* Corresponding author. Department of Mechanical Engineering, College of Engineering, University of Ha'il, Ha'il City, 81481, Saudi Arabia.
E-mail addresses: Tarekbouzennada@yahoo.fr (T. Bouzennada), kgmaatki@pnu.edu.sa (K. Ghchem), nazahi@imamu.edu.sa (N. Zahi), l.kolsi@uoh.edu.sa (L. Kolsi).

https://doi.org/10.1016/j.csite.2023.103080
Received 27 February 2023; Received in revised form 28 April 2023; Accepted 14 May 2023
Available online 15 May 2023
2214-157X/© 2023 The Authors. Published by Elsevier Ltd. This is an open access article under the CC BY-NC-ND license (http://creativecommons.org/licenses/by-nc-nd/4.0/).

techniques are applied to overcome this issue, such as placing high-conductivity fins inside PCM capsules [4] or redesigning the shape of the capsule. An experimental work using PCM annular storage has been conducted by Essa et al. [5] to determine the optimal fin structure for the heat/melt progression of a PCM. Two different fin designs were used during the experiment. The outputs indicated that the presence of fins favors the heat transfer through the PCM in all cases and that the helical fins gave a better performance in comparison with the conventional type.

The influence of PCM capsule shape on the melting velocity was investigated by Awasthi et al. [6]. The suggestion was to consider different cases of irregular wall shape; different amplitudes and sinusoidal undulations and keep the volume of the PCM constant. Briefly, the design of the capsule wall has a considerable impact during the earlier stages of the process yet during the advanced stages especially when natural convection is dominant, where the influence of irregular shape is against the desirable achievement (lowness of the melting time). In the same way, Kaviany [7] investigated the effect of a cylindrical protuberance placed on an adiabatic wall of a square cavity involving a PCM. The results revealed that changing the radius of the protuberance has a direct and significant consequence on heat distribution. In addition, PCM can be involved in the core of nanoparticles in order to increase the ability of the nanoparticles to collect further heat amount. Ghalambaz et al. [8] examined the thermal behavior of Nano-Encapsulated Phase Change Material (NEPCM) suspensions in a cylindrical cavity. NEPCM particles contain a PCM core that can absorb/release thermal energy during phase change. The results suggest that increasing the Stefan number decreases the Nusselt number during charging mode. The fusion temperature of the particle's core affects the heat transfer rate, by reducing it during the charging process and enhancing it during the discharging process. Additionally, increasing the volume fraction of NEPCM particles leads to an enhancement of the Nusselt number during the melting and solidification of the core.

In further development, the presence of high thermal conductivity nanoparticles is taken as a factor influencing the melting and heat transfer performances by dispersing them in the PCM [9,10]. Bouzennada et al. [10] observed that the thermal transmission of PCM improves by adding nanoparticles (NPs). The study examined the effect of the addition of NPs in a PCM on thermal distribution and fusion progression inside a PCM-filled cavity around a hot tube involving an HTF. It is worth mentioning that the first work including nanoparticles fused with PCM (known as NEPCM) was carried out in 2007 b y Khodadadi and Hosseinizadeh [11]. They reported that the thermal conductivity of NEPCM was enhanced in comparison to that of pure PCM, which has encouraged researchers to emphasize the significant potential of NPs in the improvement of the heat transfer. Countless published works have since proven the positive role of NPs in enhancing (increasing) heat transfer within PCMs, particularly the heat conducting mode. A numerical study conducted by Sebti et al. [12] aimed to obtain optimal results in heat transfer besides melting speed during the heat charging process in a PCM-filled annular enclosure. Various amounts of NP were dispersed in the PCM. The Results proved that the melting and heat transfer rates increase with increasing NPs volume fraction in the PCM. Rufuss et al. [13] led an experimental work that aims to improve the thermal and storage performances in a solar panel, where the absorbed heat is collected in a PCM battery. Three NPs types (TiO_2, CuO, and GO)) were mixed separately with a pure PCM (each case mixed with only one NP type) at a percentage of 3%. An improvement in thermal conductivity and a decrease in melting temperature were noted with the NEPCM compared to the pure PCM. They also recommended CuO to be the best choice of NP due to its high thermal conductivity. Tang et al. [14] found that the thermal conductivity of PCM mixed with alumina was enhanced by 12% compared to the pure PCM. Li et al. [15] proposed a novel NEPCM called Nanoparticle Paraffin-tailing ceramic composite. The presented NEPCM proved to have good chemical stability during the multiple melt-freeze cycle tests and the experimental results confirmed that this NEPCM provides a fast thermal charge/discharge rate due to its high thermal conductivity. Furthermore, Izadi et al. [16] found that nanoparticles enhance heat transfer performance, but on the other hand, they reduce flow power.

Lastly, Tofani and Tiari [17] have reviewed numerous papers regarding NEPCMs and reported that in general, NPs have been proven to improve the thermal performance of PCMs and the most commonly used NPs are Al_2O_3, copper and carbon. Many authors have indicated that NPs enhancement technique has an insignificant efficiency compared to other techniques, nevertheless, in other studies, NPs have been shown to be a cost-effective choice.

The complexity of modeling the thermal transfer during the phase change process as well as the long computational time, most of the previous studies on PCMs have been performed in 2D geometries. The 2D studies have shown satisfactory findings compared to the experimental results, allowing the use of the 2D models however it makes the studies limited.

As a result, Bondareva [18] compared the obtained data from 2D and 3D numerical simulations by considering the thermal behavior and the melting process in a PCM-filled cavity heated by an internal heater (placed on the long bottom wall). In the 3D model, all walls are adiabatic except two side walls located parallel to the heater with low temperature compared to the heater, and the 2D model is considered as the middle-cross-section of the 3D configuration. The comparison indicates that at the initial process stages, the melt level is intensive and the local Nusselt is greater using the 2D model than with the 3D one. Despite the thermal condition along the heater being constant, the 2D results are quite different from the 3D data. Numerical studies using 3D/2D models supported by experimental data were performed by Sharifi et al. [19] to investigate the melting front progression of a PCM filling a cylindrical cavity while varying the angle of the cavity. They concluded that, although experimental data were quite consistent with the 2D results, the 3D model demonstrated significant effects compared to the 2D model results, albeit at a fairly small inclination angle. Two numerical models were proposed by Soni et al. [20] and the results were compared with experimental findings. Numerical models are performed to analyze the thermal behavior and melt development of a PCM that occupies a spherical capsule. Both models are 2D configurations. One case considers the thermocouple-tube presence and the opposite with the other case. The results showed that there is an acceptable matching between the experimental outputs and the case that considers the presence of the thermocouple tube. However, the results of the other case are quite distant. It was mentioned that there is a significant influence of considering geometrical details to reduce the deviation error between the numerical results and the experimental ones. Galione et al. [21] performed 2D and 3D simulations and compared the results to the experimental findings. They considered a PCM filled spherical capsule and studied the melting process.

They concluded that there is no remarkable difference in the results of the evolution of the liquid zone between the 2D and 3D models, but the agreement of the 3D model with the experimental data is higher than the 2D one. Furthermore, there were significant differences in the flow patterns between the two models.

The present study is carried out in a cubic container (3D geometry) as shown in Fig. 1, where the PCM absorbs heat from HTF which flows along the tube that is placed at the lower area of the box. The temperature of the tube varies linearly along the tube axis (y-direction). Three different percentages of nanoparticles are used to highlight the impact on the melting process, in addition to the impact of the non-uniform thermal condition. While most numerical studies investigating the heat transfer during phase change processes utilizing PCMs are typically limited to 2D geometries, this study aims to demonstrate the importance of considering the third dimension as a significant influencer on the results. The novelty of this study lies in its focus on 3D configuration analysis, which takes into account the hypothesis that suggests a reduction in the temperature of the HTF as it flows.

The finding will be addressed in a form of comparisons of the melting rate curves/plots, temperature field, and liquid flow structure in a 3D symmetrical geometry.

2. Studied configuration and the boundary conditions

In the current study, the configuration is defined as a cuboid NEPCM-filled enclosure (*30/25/*30 mm) involving a tube (d_e/d_i=*6/*5 mm) placed in the bottom section of the enclosure that allows an HTF to flow through. The study is aiming to highlight the impact of the percentage of Al_2O_3 additive (nanoparticles) on the melting process. It is assumed that all indoor walls of the enclosure are no-slipped (u=v=w=0 m/s) and thermally insulated ($\frac{dT}{dx} = \frac{dT}{dy} = \frac{dT}{dz} = 0$) except the inner wall of the inner tube, where the temperature is varying toward the y-axis as $T(y) = T_c + \left(-5K/_Y\right)y$, where T_c = 35 K and Y is the length of the HTF-tube, besides, the no-slip condition is applied on this wall. The thermophysical properties of the selected PCM (n-Octadecane), the nanoparticles (Al_2O_3), and the inner-tube wall are presented in Table 1.

3. Mathematical model

During the current study, the heat and phase transfer phenomena are combined. The modified energy and dynamic equations, as well as the enthalpy method [23], were considered in the mathematical model. It is worth mentioning that the enthalpy method is currently the most appropriate method to tackle such studies.

The study is based on the following hypotheses.

- The liquid-NEPCM is incompressible.
- The liquid-NEPCM is Newtonian.
- The study is a 3D problem.

and the governing equations are expressed as follow:

Continuity equation

$$\frac{\partial u}{\partial x} + \frac{\partial v}{\partial y} + \frac{\partial w}{\partial z} = 0 \tag{1}$$

where u, v, and w are the velocities in x, y, and z directions, respectively.

Momentum equation

$$\frac{\partial(\rho u)}{\partial t} + u\frac{\partial(\rho u)}{\partial x} + v\frac{\partial(\rho u)}{\partial y} + w\frac{\partial(\rho u)}{\partial z} = -\frac{\partial P}{\partial x} + \mu\left[\frac{\partial^2 u}{\partial x^2} + \frac{\partial^2 u}{\partial y^2} + \frac{\partial^2 u}{\partial z^2}\right] - S_{ax} \tag{2.a}$$

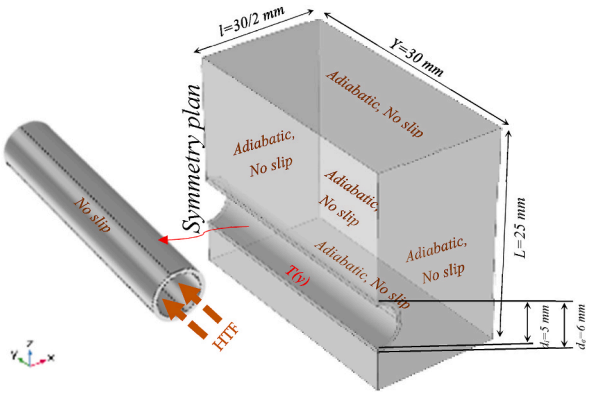

Fig. 1. 3D configuration with the boundary conditions of the study configuration.

Table 1
Thermophysical properties of n-Octadecane (PCM), inner-tube wall, and Al_2O_3 nanoparticles [22].

Properties of the Materials	PCM (n-Octadecane)		Inner-Tube Wall Copper	Nanoparticle Al_2O_3 ($d_p = 59 \times 10^{-9}$ m)
	Solid	Liquid		
Thermal conductivity, k, (W/m K)	0.39	0.157	401	36
Density, ρ, (kg/m^3)	814	770	8900	3600
dynamic viscosity, μ, (Pa s)	–	$3.8.10^{-3}$		
Thermal expansion coefficient, β, (1/K)	–	$8.5.10^{-4}$		7.810^{-6}
Specific heat, c_p, (kJ/kg K)	1.9	2.2	0.385	0.765
Melting temperature $T_m = 28$ °C and the fusion latent heat $\Delta H = 241\ kJ/kg.K$				

$$\frac{\partial(\rho v)}{\partial t}+u\frac{\partial(\rho v)}{\partial x}+v\frac{\partial(\rho v)}{\partial y}+w\frac{\partial(\rho v)}{\partial z}=-\frac{\partial P}{\partial y}+\mu\left[\frac{\partial^2 v}{\partial x^2}+\frac{\partial^2 v}{\partial y^2}+\frac{\partial^2 v}{\partial z^2}\right]-S_{ay} \tag{2.b}$$

$$\frac{\partial(\rho w)}{\partial t}+u\frac{\partial(\rho w)}{\partial x}+v\frac{\partial(\rho w)}{\partial y}+w\frac{\partial(\rho w)}{\partial z}=-\frac{\partial P}{\partial z}+\mu\left[\frac{\partial^2 w}{\partial x^2}+\frac{\partial^2 w}{\partial y^2}+\frac{\partial^2 w}{\partial z^2}\right]-S_{az}+S_b \tag{2.c}$$

Where ρ, μ, and p represent the density, dynamic viscosity and pressure respectively.

The phase-change terms (S_a) in each direction are [12]:

$$S_{ax}=-A\ \ u, S_{ay}=-A\ \ v \text{ and } S_{az}=-A\ \ w \tag{3}$$

with $A=\frac{(1-\eta)^2}{(\eta^3+10^{-3})}C$.

Where C is a constant depending on the liquid-solid interface and is set at 10^6 kg/kg/m^3·s [23].

η is the molten fraction expression used to define the cell zone, and is expressed as:

$$\eta(T)=\left\{\begin{array}{l} 0\ if\ T<(T_s=T_m-\Delta T) \\ 1\ if\ \ T>(T_l=T_m+\Delta T) \\ \dfrac{(T-T_m+\Delta T)}{2\Delta T}\ if\ \ T_l>T\geq T_s \end{array}\right\} \tag{4}$$

It is to be noted that T_l and Ts represent the temperatures in liquid and solid state, respectively. T_m is the melting point of the PCM, and ΔT is the temperature variation range ($\Delta T = 2$ K)

The Boussinesq approximation of the buoyancy force (S_b) is expressed as:

$$S_b=\rho_l\beta(T-T_m)\vec{g} \tag{5}$$

ρ_l is the density of the liquid phase, β represents the thermal expansion coefficient, and the gravity acceleration force is represented by $\vec{g}$.

Thermal equation

$$\frac{\partial(\rho H)}{\partial t}+\frac{\partial(\rho uH)}{\partial x}+\frac{\partial(\rho vH)}{\partial y}+\frac{\partial(\rho wH)}{\partial z}=k\left(\frac{\partial^2 T}{\partial x^2}+\frac{\partial^2 T}{\partial y^2}+\frac{\partial^2 T}{\partial z^2}\right) \tag{6}$$

Here H is the expression of specific enthalpy, which is formulated as follows:

$$H=h+\Delta H \tag{7}$$

where h is the sensible enthalpy, which is expressed by the following expression:

$$h=h_{ref}+\int_{T_{ref}}^{T}c_p dT \tag{8}$$

Where ΔH, h_{ref}, T_{ref}, c_p, and k represent, fusion latent heat, sensible enthalpy at $T\simeq 25°C$, reference temperature, specific heat, and thermal conductivity, respectively.

The thermophysical properties of the working material with the presence of nanoparticles are estimated as follows [22]:

Thermal conductivity at liquid and solid states

$$k_{nl}=\frac{k_{np}+2k_l-2(k_l-k_{np})\varphi}{k_{np}+2k_l-(k_l-k_{np})\varphi}k_l+5.10^4\beta_0\varphi(\rho c_p)_l\sqrt{\frac{K_bT}{\rho_{np}d_p}}f(T,\varphi) \tag{9.a}$$

$$k_{ns} = \frac{k_{np} + 2k_s - 2(k_s - k_{np})\varphi}{k_{np} + 2k_s + (k_s - k_{np})\varphi} k_s + 5.10^4 \beta_0 \varphi (\rho c_p)_l \sqrt{\frac{K_b T}{\rho_{np} d_p}} f(T, \varphi) \quad (9.b)$$

With:

$$f(T, \varphi) = (2.817.10^{-2}\varphi + 3.917.10^{-3}) \frac{T}{T_0} + (-3.0669.10^{-2}\varphi - 3.91123.10^{-3}) \quad (10)$$

Since the thermophysical properties of the working material are considered thermally steady within each physical state (liquid/Solid), in addition to these properties are being temperature-independent, the *f* function is considered at T = 320 K and T_0 = 273 K [23]

where: $\beta_0 = 8.4407(100\varphi)^{-1.07304}$, and d_p is the nano-element diameter, while the Boltzmann constant is donated as so $K_b = 1.381 \times 10^{-23}$.

density at liquid and solid states

$$\rho_{nl/s} = (1 - \varphi)\rho_{s/l} + \varphi\rho_{np} \quad (11)$$

Specific heat at liquid and solid states

$$(\rho.C_p)_{nl/s} = \varphi.(\rho.C_p)_{np} + (1 - \varphi).(\rho.C_p)_{nl/s} \quad (12)$$

Dynamic viscosity at liquid and solid states

$$\mu_{nl} = 0.983 e^{12.959\varphi} \mu_l \quad (13)$$

Latent heat

$$\Delta H_{nl} = (1 - \varphi)\Delta H \rho_l / \rho_{nl} \quad (14)$$

Thermal expansion coefficient

$$(\rho.\beta)_{nl} = \varphi.(\rho.\beta)_{np} + (1 - \varphi).(\rho.\beta)_l \quad (15)$$

Variation of density of NEPCM

$$\rho(T) = \rho_{ns} + (\rho_{nl} - \rho_{ns}).\eta(T) \quad (16)$$

Variation of c_p of NEPCM

$$c_p(T) = c_{p_{ns}} + (c_{p_{nl}} - c_{p_{ns}}).\eta(T) + D.\Delta H(T) \quad (17)$$

D represents the smoothed function of Delta Dirac during the phase change process

$D = e^{\left(-(T - T_m)^2/\Delta T^2\right)} \Big/ (\Delta T\sqrt{\pi})$ [[23]].

Variation of thermal conductivity

$$k(T) = k_{ns} + (k_{nl} - k_{ns}).\eta(T) \quad (18)$$

n, np, s and l indices refer to nano-PCM, nanoparticle, solid and liquid, respectively.

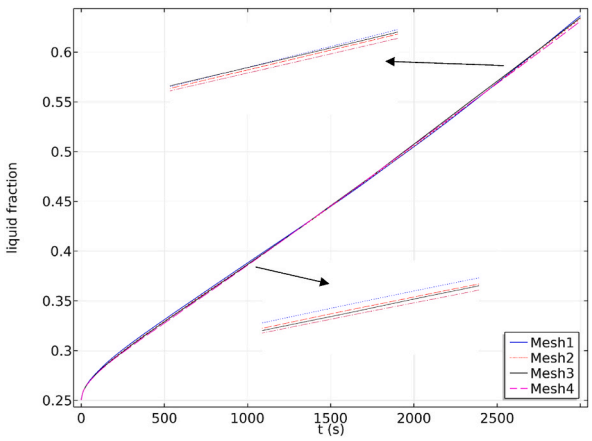

Fig. 2a. The Liquid fraction in different mesh elements; Mesh1 = 78,199, Mesh2 = 213,347, Mesh3 = 668,893, & Mesh4 = 2,865,892.

3.1. Solution procedure and mesh sensitivity

The fixed-grid method has proven its benefit in heat transfer studies during the phase change processes. In fact, no explicit treatment of the moving boundary is required using this method; in addition, it provides an additional realistic and consistent solution to the problems under study [24,25].

The solution procedure is made using the constant Newtonian iteration technique (the iterations for each time step: 6, the damping factor: 0.9). Time-dependent study feature is used while the considered running time of 3000 s where the time step is selected automatically to reach the defined error that undergoes the Backward Euler time marching method (the backward order is between 1 and 2). Note that COMSOL uses GMRES Coupled direct solver as a solver.

The mesh size is quite important in simulation, whereas knowing the accuracy of the simulation with reasonable results related to the density of the used mesh. A sensitive mesh test was performed with four different mesh sizes to avoid the influence of the mesh on the results. Fig. 2a includes the liquid fraction in different meshes (case of $\varnothing = 6\%$). It is clear that there is no significant effect of the mesh size on the results or the accuracy of the computations. This being said, mesh 3 (668,893) was selected as the optimal mesh for the study in order to avoid computational costs and the need for obtaining reasonable outputs with a clear plotting of results (the execution time of the study was about 12 days using a computing station with an Intel(R) Core(TM) i9-7980XE @ 2.60 GHz 2.59 GHz processor and 64 Gb of RAM).

The computation grid is carried out using triangle elements, as presented in Fig. 2b. The used grid is finely refined to converge easily and get satisfactory results.

3.2. Model verification

A comparison with the temporal variation of the liquid fractions presented in the work of Arasu and Mujumdar [26] is illustrated in Fig. 3a, for $\varnothing = 0$ and 5%. The development of the liquid fraction shows a good concordance between the outputs. It should be mentioned that the comparison has been performed in 2D model.

Fig. 3b compares the outputs of the used model with the results presented in Ref. [27]. The figure depicts the evolution of the liquid-solid fraction for two different thermal conditions, where the inner cylinder was exposed to two different temperatures while the outer wall remained adiabatic. The authors assumed that a PCM melts under these conditions. The figure demonstrates that the experimental/numerical outputs from the literature and the used model show a satisfactory agreement.

4. Results and discussion

4.1. Liquid fraction, isothermal-surface, and the flow structure at different time steps

Fig. 4 presents the results of the effect of NP volume fraction (at 0, 3, and 6%) on the melting process and heat transfer at various

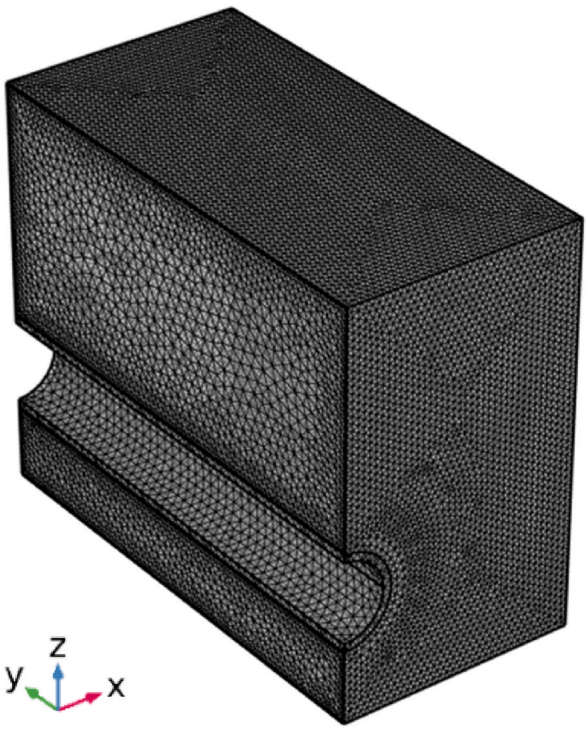

Fig. 2b. The computation grid.

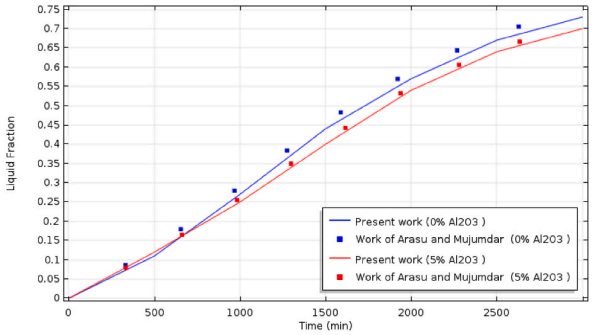

Fig. 3. a. The liquid fraction temporal variation of liquid: comparison with the numerical results of Arasu and Mujumdar [26].

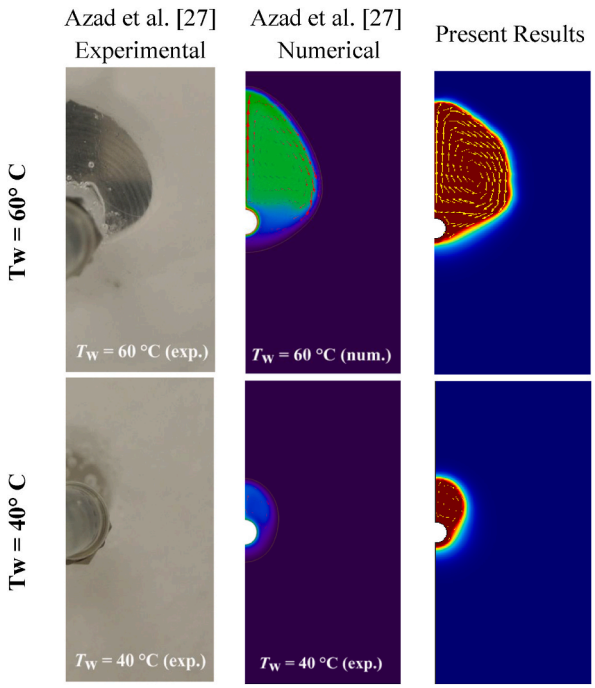

Fig. 3. b. Comparison between the simulation outputs of the used model and the numerical/experimental results reported in Ref. [27] at t = 30 min (for Tw = 60 °C and Tw = 40 °C).

times (t = 300, 1200, 1800, 2400, and 3000 s). The outcomes are illustrated in terms of the liquid-solid volume plots and isothermal-surface besides the flow structure of each NP volume fraction case.

Globally, the progression of the liquid fraction (LF) matches with the progression of the isothermal-surface on the entire melting process, i. e, the PCM-cells melt once reaching the melting point (T=T_m), and the cells or the regions that are under the melting point are in solid-state. On other hand, the arrows refer to the melt motion that is only found within the liquid part, where the liquid moves in a circular pattern because of the buoyancy force.

Taking each result individually. At t = 300 s, the molten zone starts to take an irregular shape and continues to progress with time. The molten zone takes a curved shape due to the influence of the buoyancy force created by the thermal gradation in the PCM, causing the molten-PCM moves in a round pattern indicating using the arrows.

It should be mentioned that the flow moves circumferentially around the x-direction and y-direction too as the arrows clarify. The liquid circulates over the two mentioned directions because the temperature changes in the z-direction and y-direction as well because the temperature of the tube changes along its axis. The previous lines reveal that the buoyancy force exercises in two directions where the volume of the liquid zone is wider in the foot of the tube (y = 0) and narrowing forwards. However, the influence of temperature graduation is well described in the subsequent section.

The effect of NP is observed from t = 1800 s, where the liquid volume increases as the NP percentage increases.

The isothermal-surface presents the temperature distribution in the PCM, where the temperature gradually decreases along the HTF-Tube and that was expected because the used temperature function in the y-direction of the tube. On other hand, the temperature

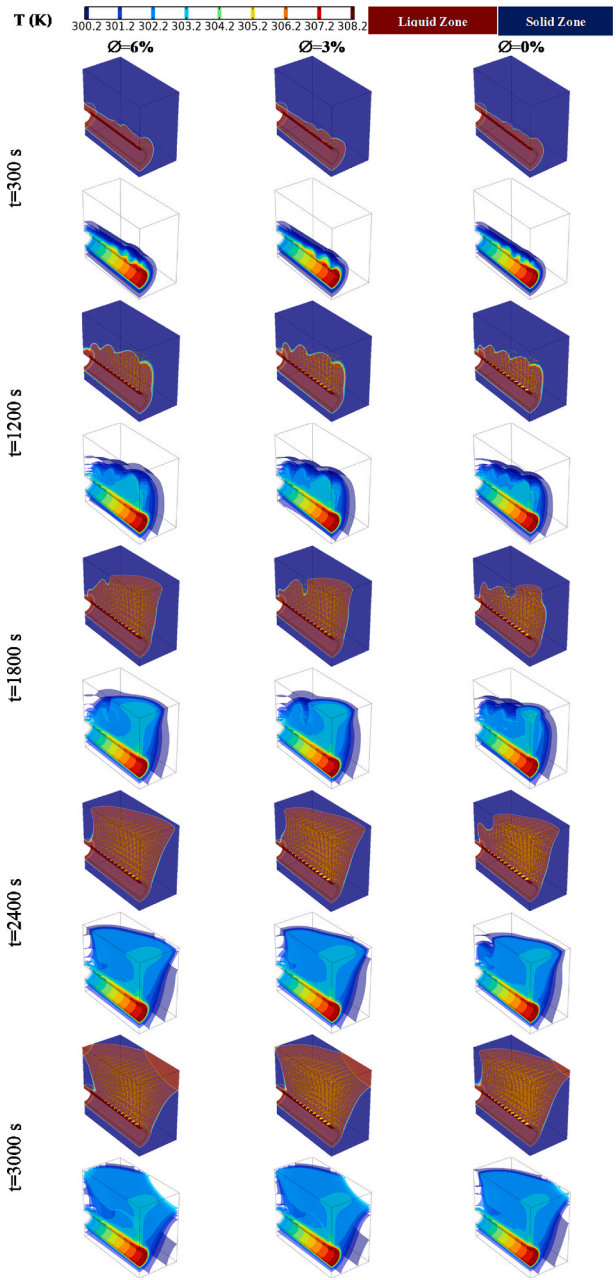

Fig. 4. Contour plots of the liquid-solid zone, the flow structure (top section), and the isothermal-surface (bottom section).

distributes from the Tube-wall forward to the sidewall in an irregular way due to the buoyancy phenomena.

Last but not least, the dominance of conduction is the main reason for the regular shape of the liquid development at the initial moment, whereas at advanced stages of the process, the liquid grows in a curved shape because the heat transfer is mainly dominated by the convection.

4.2. Influence of the temperature graduation condition

As mentioned above a non-uniform temperature condition is applied along the HTF tube. The temperature along the tube decreases gradually as presented in Fig. 5, besides the non-uniform temperature affects the melting process and the flow pattern. Fig. 6 illustrates the results at t = 3000 s for various nanoparticles volume fractions. The molten space includes arrows for a better understanding of the flow structure within the liquid region. The blue color corresponds to the solid zone. The outcomes reveal that the melting zone is wider in the area that is near the tube entrance and shrinks gradually along the tube. In addition, the molten zone is wider on the upside and is narrowing downward. This is caused by the effect of the buoyancy force that makes the melt move not only upwards. However,

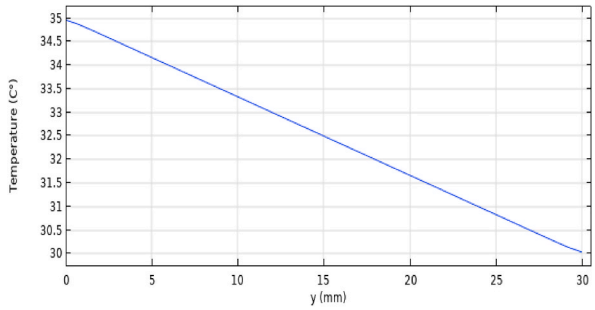

Fig. 5. Temperature variation along the tube.

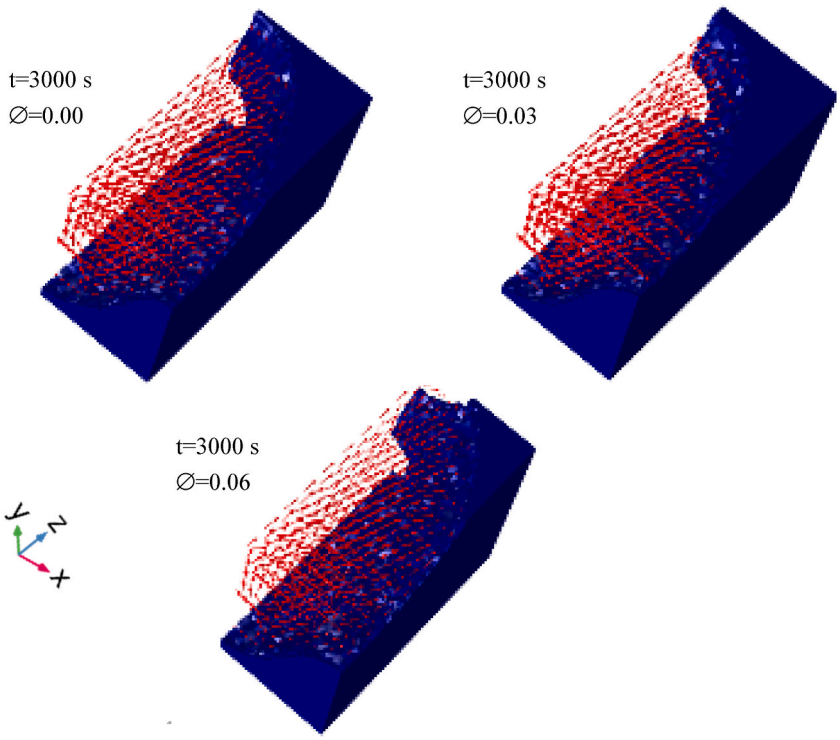

Fig. 6. Contour plots of the liquid-solid zone and the velocity field at t = 3000s for ∅ = 0.00, 0.03 and 0.06.

the melt flows toward both the transversal and vertical directions as it is observed from the arrows. The transversal fluid motion is a purely 3D result.

The reason behinds the fact that the molten zone is larger close to the entrance of the tube and the liquid flows along the tube direction is the non-uniformity of temperature condition that varies along the tube and is higher at the tube inlet.

4.3. Liquid fraction development

Fig. 7 illustrates the temporal development of the molten volume, together with the special effects of the NP percentage. It is observed that the molten progresses with time in all cases and the melting progression decreases by increasing the percentage of NP. Due to the boost of the thermal transmission, the performance of the charging process is improved by the addition of the nanoparticles. Also, the melting rate at the earlier seconds (100) of the process is the same.

4.4. Evolution of temperature in ENPCM

The temperature is evaluated in three different points inside the NEPCM region (P1 (2.5, 5,5.5), P2 (7.5, 15, 12.5), and P3 (12.5, 25, 22.5)) for all cases of Nano-percentages. Fig. 8 includes the positions of each point. Besides, Fig. 9 shows the evolution of the temperature at each point including the effect of the percentage of NP.

In P1 i. e, the bottom section, the evolution of the temperature is remarkable, the temperature strongly increases with time and constants at t = 2000 s to the end, also it is observed that the values of temperature are higher as the percentage of NP is bigger.

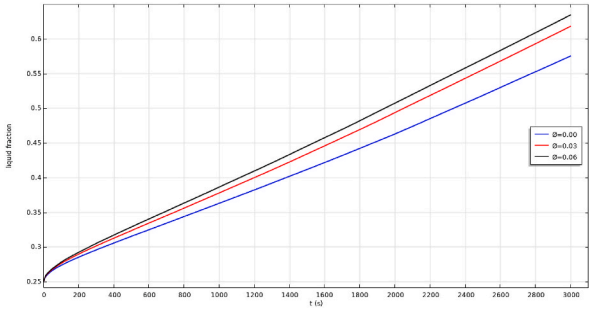

Fig. 7. The Liquid fraction development.

In P2 i. e, the middle-cross section of the cavity, the temperature increases with all percentage cases, at t < 1900 s, the values of temperature are higher as the NP percentage increases, however, in the time range 1900< t < 2700 the temperatures of the case 0% (pure PCM) is being higher where that might is caused from the additive quantity of NP that makes the motion of the liquid heaver and the heat transfer by convection becomes weaker. Afterward, the highest values are found at 6%, 3% then 0% until the last moment of the process. In P3 i. e, the top section, the temperature is constant with all cases until t = 2000 s and starts to increase slowly with the cases of 3 and 6% yet, with the case of pure PCM where the increase is barely remarkable. The slow evolution is simply because of the weak boosting of the temperature that absorbed from the hot-tube where that region needs more time to be hotter. Moreover, the added quantity of NP permitted that region to absorb heat faster whenever the NP percentage is higher.

4.5. Evolution of the stored thermal energy

Fig. 10 displays the development of the stored thermal energy by the NEPCM. The stored energy rises with time progression in all cases as shown in Fig. 8. Also, the energy amount increases with the increase in the percentage of nanoparticles. This is caused by the homogeneous heat spreading in the NEPCM due to the NP having augmented the thermal conductivity in PCM. The stored energy is computed using the integration of the following expressions over the volume cavity.

$$E = \iiint_V \rho C_p (T - T_{in}) dV \tag{19}$$

5. Conclusion

The present study is designed to examine the significant contribution of alumina NP addition, as well as its percentage, to a PCM occupied by a cuboid cavity equipped with an inner HTF tube situated in the bottom section under non-uniform temperature conditions. The principal findings of the study can be summarized as follows: the presence of NPs in the PCM increases the melting speed and stored energy by improving thermal conductivity and heat transfer. The improvement in melting speed is approximately 11% and

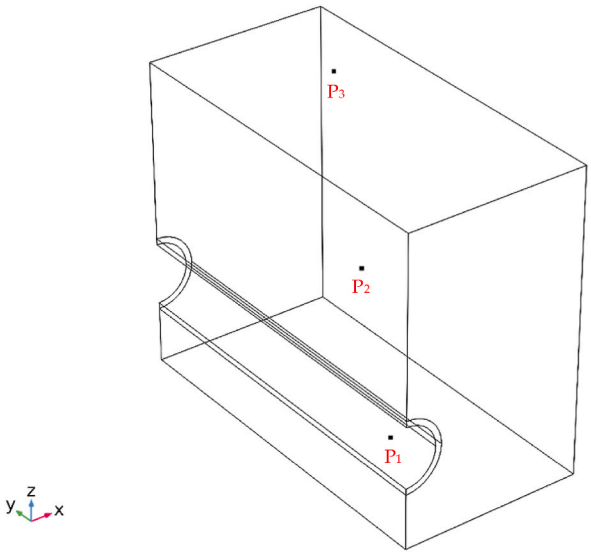

Fig. 8. The positions of each point.

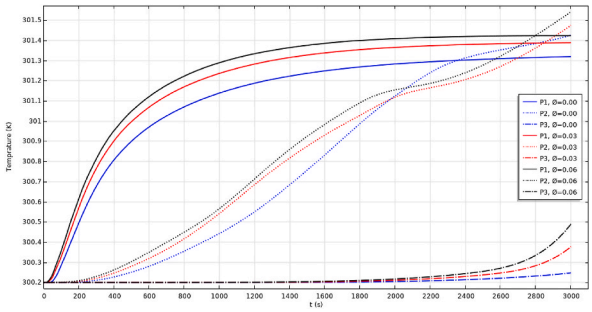

Fig. 9. Temporal variation of the temperature for the considered points for each different nanoparticle concentration.

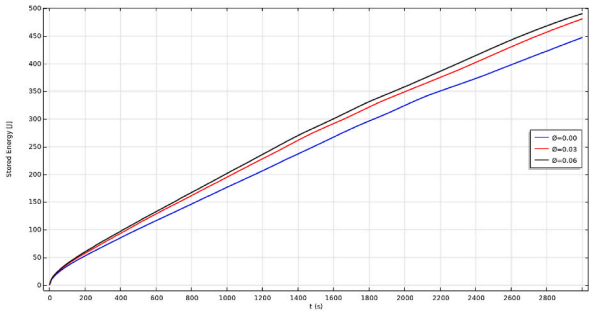

Fig. 10. Temporal evolution of the stored energy.

9.5% for 6% and 3% NP concentration, respectively, compared to the case without NPs. The stored energy improvement is evaluated at 6.5% and 9% for 3% and 6% NP concentration, respectively. The study also notes that irregular thermal conditions of the heat transfer fluid in real-world applications can affect the shape of the molten zone around the HTF tube, highlighting the importance of considering the third dimension in annular-PCM-tank systems.

Author statement

Conceptualization: Tarek Bouzennada, Kaouther Ghchem and Lioua Kolsi; Methodology/Study design: Tarek Bouzennada, Kaouther Ghchem and Nesrine Zahi. Software: Tarek Bouzennada, Muapper Alhadri and Lioua Kolsi. Validation: Tarek Bouzennada. Formal analysis: Nesrine Zahi and Muapper Alhadri. Investigation: Tarek Bouzennada and Kaouther Ghchem. Writing – original draft: All the authors. Writing – review and editing: All the authors.

Declaration of competing interest

The authors declare that they have no known competing financial interests or personal relationships that could have appeared to influence the work reported in this paper.

Data availability

No data was used for the research described in the article.

Acknowledgement

Princess Nourah bint Abdulrahman University Researchers Supporting Project number (PNURSP2023R41), Princess Nourah bint Abdulrahman University, Riyadh, Saudi Arabia.

Nomenclatures

Symbols

c_p	Specific heat, (J/kg K)
g	Gravitational acceleration, (m s^{-2})
k	Thermal conductivity, (W/m K)
P	Pressure, (Pa)

T	Temperature, (K)
T_m	Melting Point, (K)
T_l	Liquid temperature, (K)
T_s	Solid temperature, (K)
T_{in}	Initial temperature, (K)
ΔT	Transition temperature range, (K)
t	Time, (s)
u	Velocity in x-direction, (m s^{-1})
v	Velocity in y-direction, (m s^{-1})
w	Velocity in z-direction, (m s^{-1})
h	Sensible enthalpy, (kJ/kg)
H	Total enthalpy, (kJ/kg)
ΔH	Latent heat, (kJ/kg)
h_{ref}	Enthalpy reference, (kJ/kg)
D	Smoothed Delta Dirac function
S_a	Source term of porosity function, (kg.s^2.m^{-2})
S_b	Boussinesq approximation of buoyancy force, (kg.s^2.m^{-2})
C	Mushy region morphology constant, (kg/m^3.s)
dp	Nanoparticle diameter, (m)
Kb	Boltzmann constant

Greek letters

β	Thermal expansion coefficient, (K^{-1})
μ	Dynamic viscosity, (Pa.s)
κ	Permeability, (m^2)
ε	Porosity (liquid fraction)
η	Porosity function
ρ	Density (kg/m^3)
φ	Nanoparticle concentration

Subscript

s	Solid state
l	Liquid state
n	Nanoparticle
i	internal
e	external

Abbreviations

PCM	Phase Change Material
HTF	Heat Transfer Fluid
NEPCM	Nanoparticle Enhanced Phase Change Material
TES	Thermal Energy Storage
NP	Nano Particle
LF	Liquid Fraction

References

[1] Ravi Kandasamy, X.Q. Wang, A.S. Mujumdar, Application of phase change materials in thermal management of electronics, Appl. Therm. Eng. 27 (2007).
[2] D.W. Hawes, D. Feldman, D. Banu, Latent heat storage in building materials, Energy Build. 20 (1993) 77–86.
[3] F. Niu, L. Ni, Y. Yao, Y. Yu, H. Li, Performance and thermal charging/discharging features of a phase change material assisted heat pump system in heating mode, Appl. Therm. Eng. 58 (2013) 536–541.
[4] T. Bouzennada, F. Mechighel, T. Ismail, L. Kolsi, K. Ghachem, Heat transfer and fluid flow in a PCM-filled enclosure: effect of inclination angle and mid-separation fin, Int. Commun. Heat Mass Tran. 124 (2021), 105280.
[5] Mohamed A. Essa, Ibrahim Y. Rofaiel, Mohamed A. Ahmed, Experimental and theoretical analysis for the performance of evacuated tube collector integrated with helical finned heat pipes using PCM energy storage, Energy 206 (2020), 118166.
[6] A. Awasthi, B. Kumar, H.H. Nguyen, S.S. Lee, J.D. Chung, Effect of sinusoidal cylindrical surface of PCM on melting performance, J. Mech. Sci. Technol. 34 (8) (2020) 3395–3402.
[7] M. Kaviany, Effect of a Protuberance on Thermal Convection in a Square Cavity, 1984.
[8] M. Ghalambaz, S.A.M. Mehryan, N. Mashoofi, A. Hajjar, A.J. Chamkha, M. Sheremet, O. Younis, Free convective melting-solidification heat transfer of nano-encapsulated phase change particles suspensions inside a coaxial pipe, Adv. Powder Technol. 31 (11) (2020) 4470–4481.
[9] A.V. Arasu, A.S. Mujumdar, Numerical study on melting of paraffin wax with Al2O3 in a square enclosure, Int. Commun. Heat Mass Tran. 39 (2012) 8–16.

[10] Tarek Bouzennada, et al., Numerical simulation of the impact of the heat source position on melting of a nano-enhanced phase change material, Nanomaterials 11 (6) (2021) 1425.
[11] J.M. Khodadadi, S.F. Hosseinizadeh, Nanoparticle-enhanced phase change materials (NEPCM) with great potential for improved thermal energy storage, Int. Commun. Heat Mass Tran. 34 (5) (2007) 534–543.
[12] S.S. Sebti, M. Mastiani, S. Kashani, H. Mirzaei, A. Sohrabi, Numerical study of melting in an annulur enclosure filled with nano-enhanced phase change material, Therm. Sci. 19 (3) (2015) 1067–1076.
[13] D.D.W. Rufuss, L. Suganthi, S. Iniyan, P.A. Davies, Effects of nanoparticle-enhanced phase change material (NPCM) on solar still productivity, J. Clean. Prod. 192 (2018) 9–29.
[14] Y. Tang, D. Su, X. Huang, G. Alva, L. Liu, G. Fang, Synthesis and thermal properties of the MA/HDPE composites with nano-additives as form-stable PCM with improved thermal conductivity, Appl. Energy 180 (2016) 116–129.
[15] R. Li, Y. Zhou, X. Duan, Nanoparticle enhanced paraffin and tailing ceramic composite phase change material for thermal energy storage, Sustain. Energy Fuels 4 (9) (2020) 4547–4557.
[16] M. Izadi, N.M. Maleki, I. Pop, S.A.M. Mehryan, Natural convection of a hybrid nanofluid subjected to non-uniform magnetic field within porous medium including circular heater, Int. J. Numer. Methods Heat Fluid Flow (2019).
[17] K. Tofani, S. Tiari, Nano-enhanced phase change materials in latent heat thermal energy storage systems: a review, Energies 14 (13) (2021) 3821.
[18] Bondareva Nadezhda, Numerical simulation of natural convection melting in 2D and 3D enclosures, J. Therm. Eng. 5 (1) (2019) 51–61.
[19] Nourouddin Sharifi, et al., Three-dimensional PCM melting in a vertical cylindrical enclosure including the effects of tilting, Int. J. Heat Mass Tran. 65 (2013) 798–806.
[20] V. Soni, A. Kumar, V.K. Jain, Modeling of PCM melting: analysis of discrepancy between numerical and experimental results and energy storage performance, Energy 150 (2018) 190–204.
[21] P.A. Galione, O. Lehmkuhl, J. Rigola, A. Oliva, Fixed-grid numerical modeling of melting and solidification using variable thermo-physical properties–Application to the melting of n-Octadecane inside a spherical capsule, Int. J. Heat Mass Tran. 86 (2015) 721–743.
[22] N.S. Bondareva, B. Buonomo, O. Manca, M.A. Sheremet, Heat transfer inside cooling system based on phase change material with alumina nanoparticles, Appl. Therm. Eng. 144 (2018) 972–981, https://doi.org/10.1016/j.applthermaleng.2018.09.002.
[23] Tarek Bouzennada, et al., Study of the usability of sinusoidal function heat flux based on enthalpy-porosity technique for PCM-related applications, J. Therm. Anal. Calorimetry (2020) 1–16.
[24] V.R. Voller, C. Prakash, A fixed grid numerical modelling methodology for convection-diffusion mushy region phase-change problems, Int. J. Heat Mass Tran. 30 (1987) 1709–1719.
[25] K. Kant, A. Shukla, A. Sharma, P.H. Biwole, Melting and solidification behaviour of phase change materials with cyclic heating and cooling, J. Energy Storage 15 (2018) 274–282.
[26] A.V. Arasu, A.S. Mujumdar, Numerical study on melting of paraffin wax with Al2O3 in a square enclosure, International Com-munications in Heat Mass Transf. 39 (2012) 8–16 (PDF) Numerical Simulation of the Impact of the Heat Source Position on Melting of a Nano-Enhanced Phase Change Material. Available.
[27] M. Azad, D. Dineshan, D. Groulx, A. Donaldson, Melting of Phase Change Materials in a cylindrical enclosure: parameters influencing natural convection onset, in: Proceedings of the 4th International Forum on Heat Transfer, IFHT2016, Sendai International Center, Sendai, Japan, 2016, November, pp. 2–4.